P1.37 ARE THERE WEATHER HOLES? AN OBJECTIVE ANALYSIS

Matthew D. Parker*
University of Nebraska–Lincoln, Lincoln, Nebraska

Jason C. Knievel
National Center for Atmospheric Research, Boulder, Colorado

1. INTRODUCTION

Most meteorologists are acquainted with the notion of a weather hole, that is, a location that storms often barely miss or near which approaching storms often dissipate. Put more plainly, a weather hole is a location that receives less interesting weather than does its surrounding area. In our experience, many meteorologists and lay weather enthusiasts think that they live in weather holes. We have generally believed that such people simply enjoy experiencing interesting weather, are memorably disappointed whenever it misses them, and eventually conclude that their location is subject to some kind of meteorological disfavor. The recent availability of multiple years' worth of national radar composites from the WSR-88D network makes it feasible to address objectively whether the concept of a weather hole is reasonable, and to evaluate the degree to which selected sites may be weather holes (or even weather hot spots).

Our study is an effort to satisfy our curiosity about rumored weather holes while simultaneously demonstrating one method for constructing local climatographies of convective echoes using a comparatively new, and readily available, dataset from the WSR-88D network. In the future, radar-based climatographies may prove to be very powerful, important tools for forecasting thunderstorms and for quantifying the risks that thunderstorms pose to society.

2. DATA AND METHODS

2.1 Radar

Our analyses incorporate NOWrad™ national composites, or summaries, of WSR–88D reflectivity data for six years: 1996–2000 and 2002. (We omitted data from 2001 because they were missing for 1 January–3 May.) The radar data have a pixel size no larger than 2 km × 2 km and represent the highest measured reflectivity in each pixel's vertical column over a 15–minute period, binned in 5–dBZ increments. The data cover most of the conterminous U.S., nominally at 15–minute intervals. In addition to the actual reflectivities, we also specifically recorded the number and locations of echoes that exceed 40 dBZ in each 15–minute summary. For the purposes of commentary in this article, we henceforth call each echo that is $\geq$ 40 dBZ a *storm element* (or, more briefly, a *storm*), and call each 15–minute radar summary a *time*.

2.2 Targets

Because some meteorologists suspect they live in weather holes, we identified for detailed study 21 target cities with large meteorological communities, selected to represent all regions of the United States roughly equally (Fig. 1 and Table 1; note that this and all other tables are in the appendix). We then used for comparison a random number generator's selections of 50 latitude/longitude pairs within the conterminous United States (dots in Fig. 1). Because radar coverage was incomplete at some of the targets, and because we anticipated significant regional variations in the radar statistics, we isolated from the 71 total targets 2 additional subsets: 1) targets with good radar coverage only ("GOOD," comprising 54 targets of 15 meteorological cities and 39 random points), and 2) targets within the region bounded by 30N, 104W, 49N, and 87.5W, which roughly corresponds to the Great Plains ("PLAINS," comprising 27 targets of 8 meteorological cities and 19 random points within the green box in Fig. 1). The targets included in each subset are denoted in Table 1.

2.3 Statistics

We present in this article statistics and plots of radar data over several square arrays, centered on the centerpoint of each target city, that represent familiar geopolitical entities. A square that is 274 km × 274 km = 75076 km^2 approximates the size of a typical National Weather Service county warning area (CWA). A square that is 54 km × 54 km = 2916 km^2 approximates the size of a typical county in the U.S. A square that is 14 km × 14 km = 196 km^2 approximates the size of a moderately large city. In this article, points within the

* *Corresponding author address:* Matthew D. Parker, Department of Geosciences, University of Nebraska–Lincoln, 214 Bessey Hall, Lincoln, NE 68588–0340. E-mail: parker@updraft.unl.edu

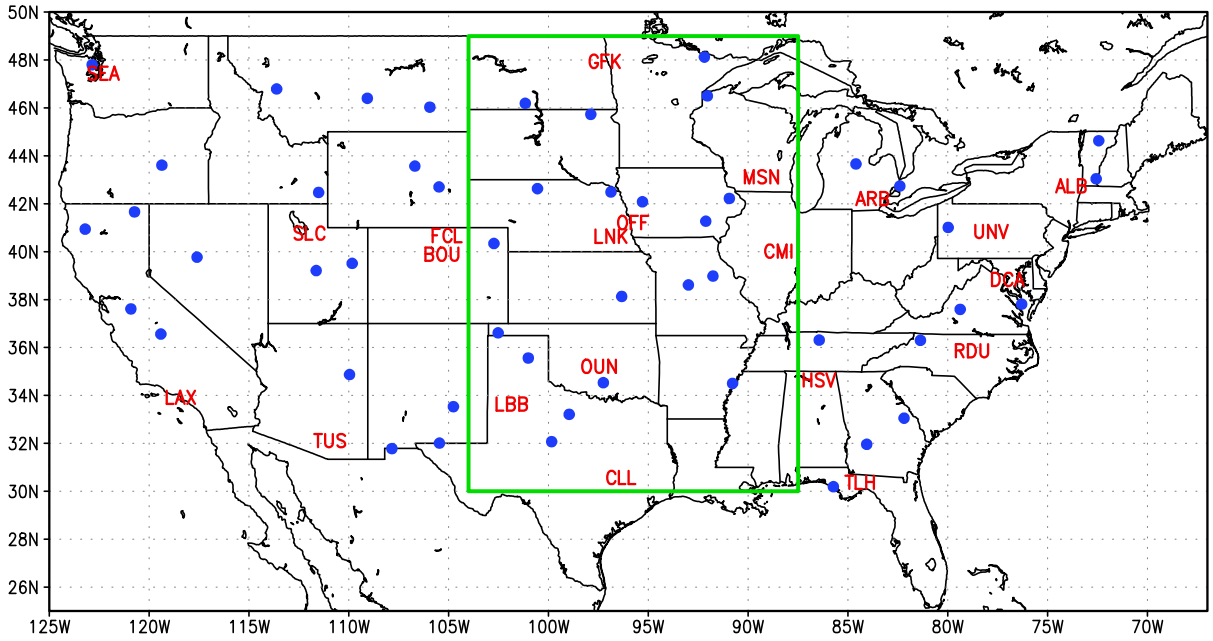

Figure 1: Target sites analyzed in this study: red 3–letter identifiers represent 21 locations with large meteorological communities, chosen for detailed study (cf. Table 1); blue dots represent 50 randomly selected comparison targets. Green box denotes region for “PLAINS” subset.

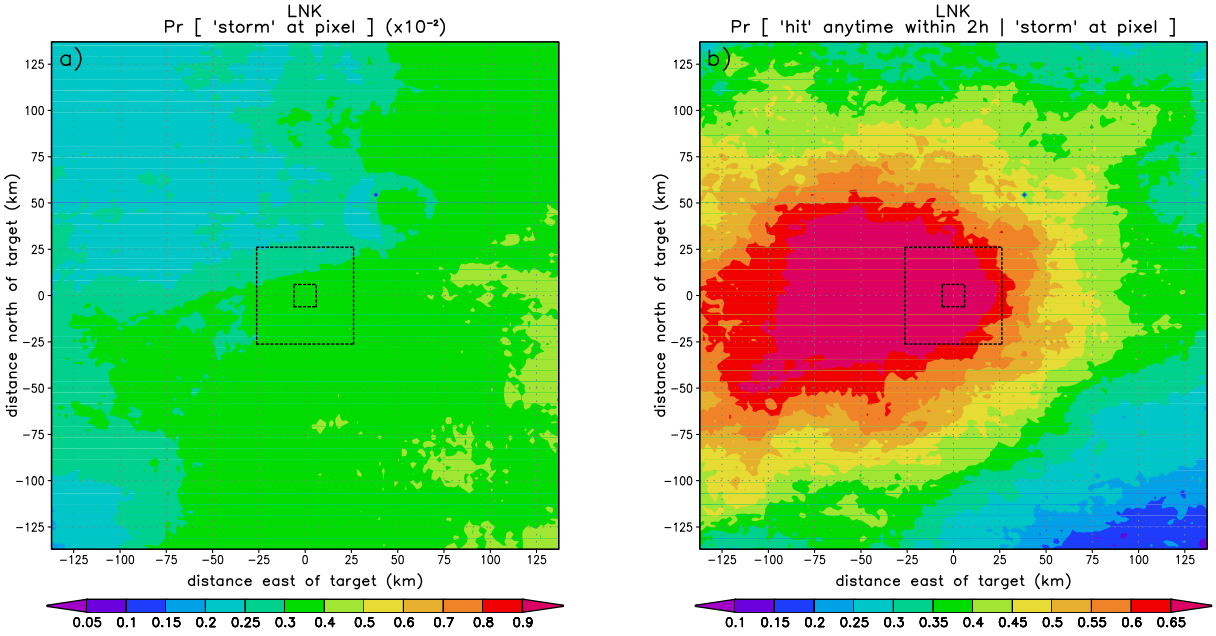

Figure 2: Plan view chart of a) Pr_{storm} (plotted values have units of 10^{-2}) and b) $Pr_{anyhit|storm}$ for Lincoln, Nebraska during the 6 years of this study. Lincoln is located in the center of the diagram ($x = 0,\ y = 0$). The smallest box outlines LNK’s “city”; the larger box outlines LNK’s ”county”; the full plot encompasses LNK’s “CWA”. The statistical computations are explained in the text.

square arrays are identified by their locations relative to a target pixel, which has coordinates of $x = 0$, $y = 0$. Our results are based on four statistical formulae. First, for the binary "storm" variable i_{40}, defined by

$$i_{40} = \begin{cases} 1 \\ 0 \end{cases} \text{ when } \begin{matrix} dBZ \geq 40 \\ dBZ < 40 \end{matrix} , \quad (1)$$

we computed the following two statistics at each point in the target array for the n times in the 6–year sample:

$$\mathrm{Pr}_{\mathrm{storm}}(x, y) = \frac{1}{n} \sum_{t=1}^{n} i_{40}(x, y, t) , \quad (2)$$

which is the probability that point (x, y) had a storm at a randomly selected time, and

$$\mathrm{Pr}_{\mathrm{hit|storm}}(x, y, \Delta t) = \frac{\sum_{t=1}^{n} i_{40}(x, y, t) \cdot i_{40}(0, 0, t + \Delta t)}{\sum_{t=1}^{n} i_{40}(x, y, t)}, \quad (3)$$

which is the normalized probability that, when a storm at point (x, y) occurred, a storm at the target also occurred Δt later (with Δt, the lag time, taken in 15–min intervals between 0 and 120 min). In order to summarize all of the information represented by the two-dimensional $\mathrm{Pr}_{\mathrm{hit|storm}}$ field for each lag time, we computed the overall probability that a storm at point (x, y) was followed by a storm at the target *at any time* during the subsequent 2 hours:

$$\mathrm{Pr}_{\mathrm{anyhit|storm}}(x, y) = 1 - \left\{ \left[1 - \mathrm{Pr}_{\mathrm{hit|storm}}(x, y, \Delta t = 15\mathrm{min}) \right] [...] \left[1 - \mathrm{Pr}_{\mathrm{hit|storm}}(x, y, \Delta t = 120\mathrm{min}) \right] \right\} . \quad (4)$$

2.4 Objective definitions of a weather hole and hot spot

We consider a weather hole to satisfy two primary criteria: it must have had markedly fewer storms than its surroundings, and it must have been disproportionately missed by approaching storms. A hot spot satisfies the converse criteria.

The first criterion, whether a target received markedly fewer or more storms than its surroundings, is quantified by $\mathrm{Pr}_{\mathrm{storm}}$. We computed $\mathrm{Pr}_{\mathrm{storm}}$ for each target, and for each pixel in its surrounding county and CWA. The mean $\mathrm{Pr}_{\mathrm{storm}}$ in the GOOD targets' CWAs was 2.85×10^{-3} (i.e., roughly 25 hours of storminess per year), and the mean standard deviation among the pixels within the CWA was 6.00×10^{-4}, which was about 20%. We set the threshold for a potential hole or hot spot at one half of this standard deviation, so a target was a potential hole if its city-wide and/or county-wide mean $\mathrm{Pr}_{\mathrm{storm}}$ was either 3.00×10^{-4} or 10% lower than in its surrounding CWA, whichever was easier to satisfy. The converse defines a potential hot spot.

The second criterion, whether a target was disproportionately missed by approaching storms, is quantified by $\mathrm{Pr}_{\mathrm{anyhit|storm}}$. We computed the azimuthally averaged values of $\mathrm{Pr}_{\mathrm{anyhit|storm}}$ for five radii (20, 40, 60, 80, and 100 km) at all 71 targets. If a target's value of $\mathrm{Pr}_{\mathrm{anyhit|storm}}$ fell within the bottom quartile of the distribution for any 3 of the 5 sampled radii, the target was considered a potential hole. The threshold was the converse for a potential hot spot. Statistics for the meteorological cities were evaluated against those for each of the group(s) (all, GOOD, and PLAINS) to which the cities belonged.

These two criteria for holes and hot spots were both necessary because sites with low or high mean values of $\mathrm{Pr}_{\mathrm{storm}}$ were not necessarily holes or hot spots. For example, many apparent holes may simply have been located within regions where storms were unusually scarce compared to elsewhere in the nation. These may be dull places for a meteorologist to live, but they were not "missed" by storms on the regional scale in any recurring way.

3. STATISTICAL RESULTS

3.1 A typical target

Because it was a typical target, LNK serves to demonstrate the diagnostic capabilities of our statistics. LNK was neither a local minimum nor a significant local maximum in $\mathrm{Pr}_{\mathrm{storm}}$ (Fig. 2a and Table 2). The predominant signal of $\mathrm{Pr}_{\mathrm{storm}}$ increasing from northwest to southeast (Fig. 2a) indicates that, on average, thunderstorms were slightly more common in the southeastern part of LNK's CWA than in the northwestern part. LNK's city average $\mathrm{Pr}_{\mathrm{storm}}$, 3.32×10^{-3}, was higher than the GOOD population average. However, LNK was not a hot spot because it did not receive significantly more thunderstorms than what is suggested by the region's field of $\mathrm{Pr}_{\mathrm{storm}}$.

Judging from the LNK CWA's $\mathrm{Pr}_{\mathrm{anyhit|storm}}$ (Fig. 2b), thunderstorms arrived at LNK most frequently from the west and west–southwest, and very rarely from the southeast. The slight elongation of the major axis in LNK's upstream maximum in $\mathrm{Pr}_{\mathrm{anyhit|storm}}$ further suggests the recurrence of frontal convective bands and/or MCSs that most frequently have a southwest–northeast orientation. LNK also did not qualify as either a hole or hot spot based upon its azimuthaly averaged values of $\mathrm{Pr}_{\mathrm{anyhit|storm}}$ at the radii considered (cf. Tables 3 and 4). During the six years studied, storms within 100 km to the west–northwest, west, and west–southwest of LNK were followed within 2 hours by a storm at LNK at least two thirds of the time (Fig. 2b).

3.2 A weather hole

The lone weather hole among the 21 meteorological targets was GFK (Fig. 3). The regional $\mathrm{Pr}_{\mathrm{storm}}$ decreased from south to north in Grand Forks' CWA. Although it may not be obvious at first glance that GFK's local $\mathrm{Pr}_{\mathrm{storm}}$ was significantly lower than that of the surrounding CWA (as documented in Table 2), Fig. 3a does reveal that GFK resides within a corridor where $\mathrm{Pr}_{\mathrm{storm}}$ was low compared to points farther east and west. The minimum in $\mathrm{Pr}_{\mathrm{storm}}$ overlays the Red River Valley, in which Grand Forks is centered. Because the gradients in elevation (not shown) and in $\mathrm{Pr}_{\mathrm{storm}}$ correspond so well, we infer that the Red River Valley is comparatively inhospitable to thunderstorms, perhaps because of local solenoidal circulations induced by the terrain.

Also relevant to GFK's classification as a hole are its comparatively low values of $\mathrm{Pr}_{\mathrm{anyhit|storm}}$ (Fig. 3b, Table 4). In comparing GFK's $\mathrm{Pr}_{\mathrm{anyhit|storm}}$ to LNK's (Fig. 2b) it is clear that although thunderstorms only a few tens of km west of GFK were followed by storms at the target at a similar rate, storms from other directions hit GFK far less frequently. This led to the comparatively small azimuthally averaged values for $\mathrm{Pr}_{\mathrm{anyhit|storm}}$ at GFK (Table 4) and its qualification as a hole. This may in part be attributable to a propensity for thunderstorms to arrive at GFK almost exclusively from the west, coupled with the unfavorability of the Red River Valley, as mentioned above.

3.3 A weather hot spot

The lone weather hot spot among the 21 meteorological targets was TLH (Fig. 4). In TLH's CWA, values of $\mathrm{Pr}_{\mathrm{storm}}$ decreased southward (i.e., seaward) and were largest roughly 20 km from the coast (in Fig. 4a, the coastline is roughly along the southern part of shaded region with $\mathrm{Pr}_{\mathrm{storm}} > 0.7\times10^{-2}$, approximately 40 km south of TLH). TLH lies on the northern fringe of these maxima, which were almost certainly caused by the recurring diurnal convection associated with the sea–breeze front (e.g., Byers and Rodebush, 1948; Frank et al., 1967). $\mathrm{Pr}_{\mathrm{storm}}$ decreased farther inland, especially to the northeast. As a result, it is evident from Fig. 4a that TLH's county (and city) mean $\mathrm{Pr}_{\mathrm{storm}}$ were relatively high compared to values in many other parts of the CWA. For this reason TLH qualified as a weather hot spot (Table 2). The maxima in $\mathrm{Pr}_{\mathrm{storm}}$ south and southeast of TLH illustrate an important point (Fig. 4a). Hot spots need not have been the single most frequent sites of thunderstorms in their CWA areas. Although TLH was a hot spot, a few other locations in its CWA received even more storms.

TLH's regional plot of $\mathrm{Pr}_{\mathrm{anyhit|storm}}$ (Fig. 4b) is in many ways similar to that for the typical site, LNK (Fig. 2b). The important difference is that, around TLH, high values of $\mathrm{Pr}_{\mathrm{anyhit|storm}}$ covered a much larger azimuthal range. TLH's average values were in the upper quartile of targets at all five radii considered (cf. Tables 3 and 4), which helps establish TLH as a hot spot. High values of $\mathrm{Pr}_{\mathrm{anyhit|storm}}$ southwest of TLH likely were a product of enhanced convergence associated with the sea breeze along the convex coastline of the Apalachicola Peninsula. High values in other directions arose from the frequent, widespread thunderstorms that typify summer weather in Florida (e.g., Byers and Rodebush, 1948).

3.4 Interannual variability

Not only did distributions of thunderstorms vary spatially among targets, the distributions also varied temporally among years. The variations were no doubt partly a response to changes in regimes of the synoptic and planetary flows that affect the frequency and degree of organization of convection.

LNK's two most outlying years (1996 and 2000) serve as useful examples. In 1996, LNK was a hot spot according to our criteria for the 6-year dataset. (The criteria would have been different for individual years). LNK's $\mathrm{Pr}_{\mathrm{storm}}$ was higher than in areas to its southwest, west, northwest, north, and northeast (Fig. 5a), and the city was hit by a fairly high proportion of upstream storms (cf. Figs. 2b and 5b), especially from the west and southwest. In 2000, LNK was a hole according to our criteria for the 6-year dataset. The city's $\mathrm{Pr}_{\mathrm{storm}}$ was lower than in much of its CWA (e.g. the quasi–annular ring of elevated $\mathrm{Pr}_{\mathrm{storm}}$ at a radius of approximately 100 km in Fig. 6a), and LNK had quite low upstream values of $\mathrm{Pr}_{\mathrm{anyhit|storm}}$ in nearly all directions (cf. Figs. 2b and 6b). LNK would have also qualified as a hot spot in 2002. In the remaining three years it was neither a hot spot nor a hole, and had statistics more similar to the means listed in Fig. 2.

It is also worthwhile to consider the interannual variability among targets that qualified as weather hot spots and holes over the 6 years studied. GFK, a hole, had lower values of $\mathrm{Pr}_{\mathrm{storm}}$ than its surrounding CWA in five of the six years, and would have qualified as a hole (including the $\mathrm{Pr}_{\mathrm{anyhit|storm}}$ criterion) in four of the six years. GFK was never a hot spot. TLH, a hot spot, had higher values of $\mathrm{Pr}_{\mathrm{storm}}$ than its surrounding CWA in five of the six years, would have qualified as a hot spot in two of the six years, and almost qualified in two additional years. TLH was never a hole. For the 6 years we studied, extreme periods evened out for most of the targets. Only for those that qualified as holes and hot spots, GFK and TLH, did extreme distributions of thunderstorms tend to persist from year to year.

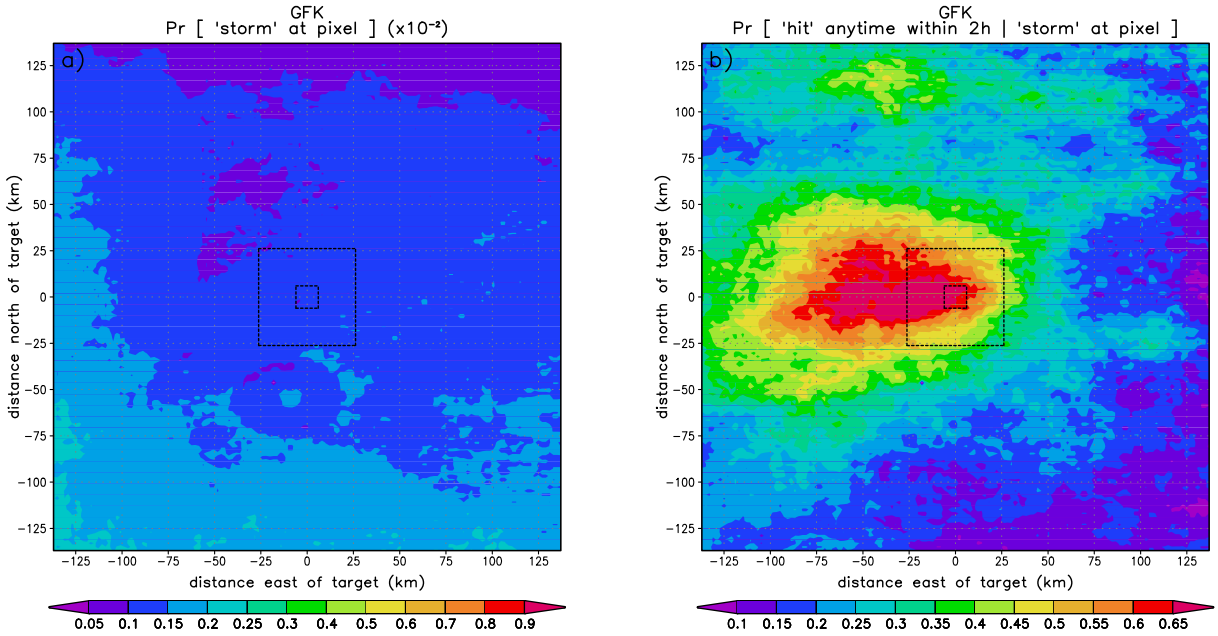

Figure 3: Same as Fig. 2 except for Grand Forks, North Dakota.

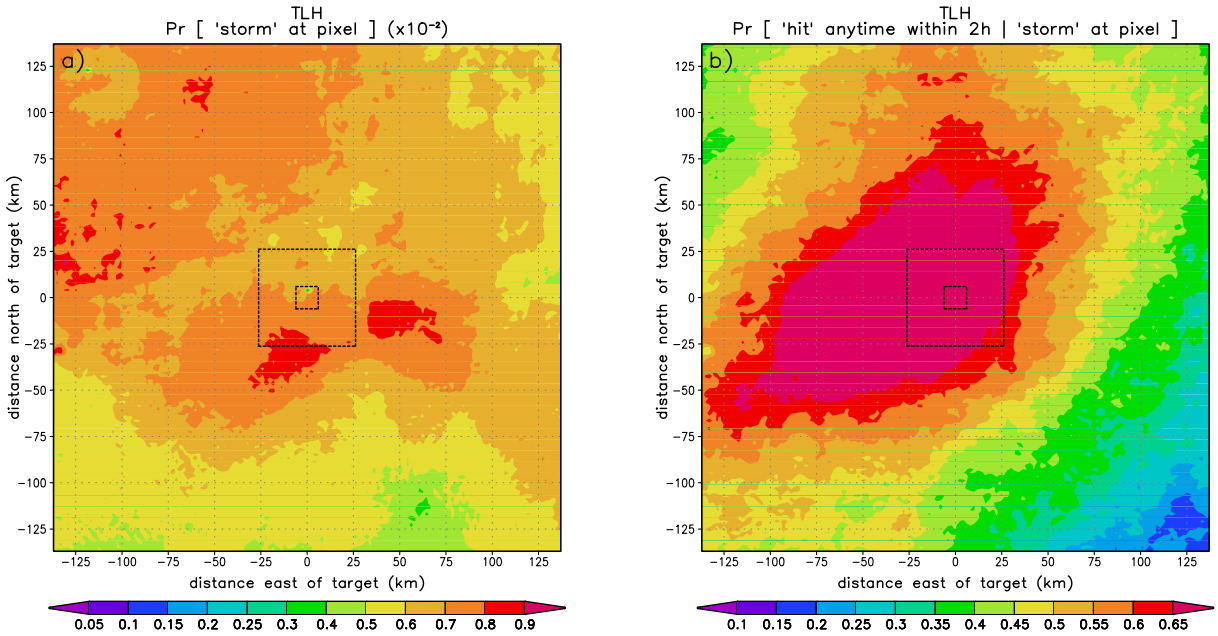

Figure 4: Same as Fig. 2 except for Tallahassee, Florida.

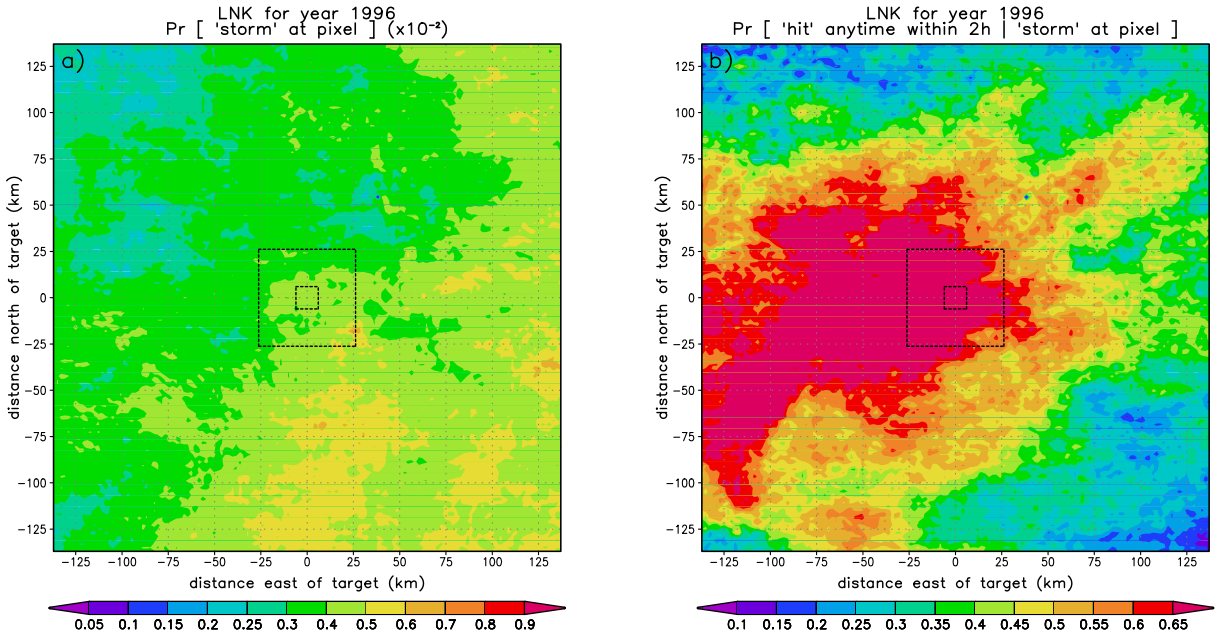

Figure 5: Same as Fig. 2 except only including data from 1996, the year in which Lincoln was most like a thunderstorm hot spot. The mean areal values for $\mathrm{Pr}_{\mathrm{storm}}$ were: city, 4.35×10^{-3}; county, 4.11×10^{-3}; CWA, 3.95×10^{-3}.

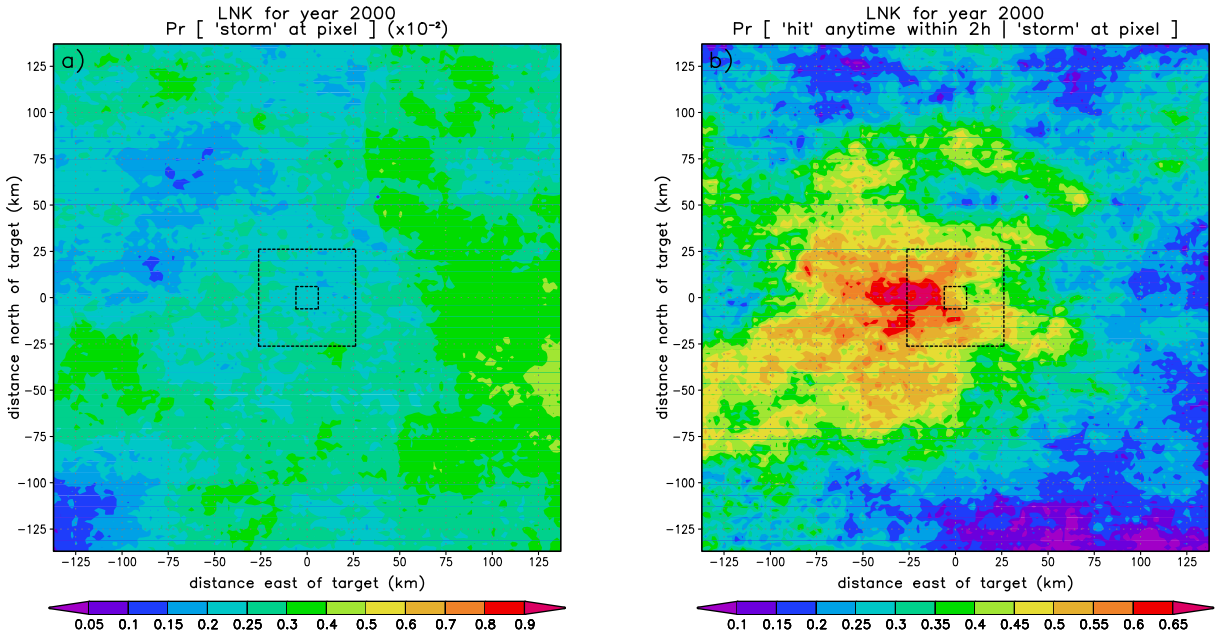

Figure 6: Same as Fig. 2 except only including data from 2000, the year in which Lincoln was most like a thunderstorm hole. The mean areal values for $\mathrm{Pr}_{\mathrm{storm}}$ were: city, 2.25×10^{-3}; county, 2.40×10^{-3}; CWA, 2.64×10^{-3}.

3.5 *Affects of terrain and poor radar coverage*

Statistics for TUS (Fig. 7) reveal some of the difficulties introduced by complicated terrain that blocks radar beams. The primary regional radar is relatively unimpeded in its observations of TUS itself, but the radar beam is mostly blocked by mountain ranges to its southwest, northeast, east and southeast (Fig. 7a).

Such blocking presented several difficulties. First, it is unclear whether regions of very high $\mathrm{Pr}_{\mathrm{storm}}$ (e.g., at $x = 15$ km $y = 30$ km in Fig. 7a) corresponded to virtually stationary orographic thunderstorms or to ground returns from terrain (Fig. 7b). Second, owing to beam blockage, there was no information in the lee of the nearby ranges (as discussed above), so that comparing TUS's $\mathrm{Pr}_{\mathrm{storm}}$ with that of its CWA has very little meaning. Third, owing to the paucity of thunderstorm echoes, $\mathrm{Pr}_{\mathrm{anyhit|storm}}$ in the radar voids was excessively noisy and unreliable, especially in the southwestern part of the Tucson CWA (Fig. 7b). For these reasons, although we gained some limited insight into the regional behavior of thunderstorms at targets with poor radar coverage, we excluded them from our core analyses.

4. SYNTHESIS AND INTERPRETATION

As mentioned, GFK was a weather hole, as were six of the random targets. TLH was a hot spot, as were another six of the random targets. Three of the meteorological targets met only the first criterion for a hole: CLL, HSV, and UNV. Two met only the second criterion: FCL and SEA. Eight targets met only the first criterion for a hot spot: ARB, BOU, FCL, LAX, RDU, SEA, SLC, and TUS. Five met only the second criterion: CLL, HSV, MSN, OFF, and OUN.

Our study suggests that many meteorological communities reputed to be convective weather holes are not much different from most other places. Holes and hot spots in this study were not more frequent among the meteorological targets than they were among the random targets. There are several possible statistical and physical reasons.

First, communities of meteorologists tend to be reasonably close to operational radars. Although we did not attempt to quantify the effects of varying distance from a radar, we did not notice any systematic increases or decreases in $\mathrm{Pr}_{\mathrm{storm}}$ or $\mathrm{Pr}_{\mathrm{anyhit|storm}}$ as a function of range from individual radar sites. There are several pixels whose anomalous values revealed the presence of persistent clutter (e.g. by a telecommunications antenna near a radar), but excluding these pixels had very little affect on the statistics, which were averaged over areas much larger than one pixel.

In addition to the possible artificial influence of distance from a radar, there may also be real, physical reasons that many meteorological targets have high values of $\mathrm{Pr}_{\mathrm{storm}}$ and $\mathrm{Pr}_{\mathrm{anyhit|storm}}$. For example, meteorological communities tend to be in cities, near which convection may be enhanced. We did not attempt to quantify effects of urban heat islands, but other researchers have shown that thunderstorms sometimes are enhanced downwind of urban areas (e.g. Changnon and Huff, 1986; Rozoff et al., 2003). It is not clear whether this helps to account for the scarcity of meteorological weather holes.

Additionally, there are clearly regional differences in convective climates among the targets. Widespread convective episodes, particularly involving mesoscale convective systems (MCSs), have expansive areas of echoes ≥ 40 dBZ. Hence, when a large MCS crossed a target site's CWA, there were three statistical effects. The first effect was that $\mathrm{Pr}_{\mathrm{storm}}$ was much more homogeneous for the CWA than it would have been during an outbreak of isolated convective cells. The second effect is that, for any given pixel, $\mathrm{Pr}_{\mathrm{anyhit|storm}}$ likely was higher for MCSs, which are often longest in the direction perpendicular to their motion, are long-lived, and are comparatively self-sustaining. The third effect is that, provided a target site was indeed hit by an MCS, the pixels that received non–zero contributions to $\mathrm{Pr}_{\mathrm{anyhit|storm}}$ were more widespread, owing to an MCSs' size and speed. Because many of the meteorological targets with GOOD data in this study were located in the central U.S., where MCSs are common (e.g., Maddox et al., 1986; Augustine and Howard, 1991), this may also partly explain the rareness of meteorological weather holes.

Whether it is physically attributable to urban effects, the frequency of MCSs, or to some other influence, our study suggests that most meteorologists do not actually live in weather holes. Coupled with this result, it is meaningful that there are temporal variations in the statistics. Targets that were classified as holes or hot spots had *consistently* lower (or higher) values of $\mathrm{Pr}_{\mathrm{storm}}$ and $\mathrm{Pr}_{\mathrm{anyhit|storm}}$ from year to year. The fact that some targets had hole–like properties in some years and hot-spot–like properties in other years is evidence that meteorologists' short–term observations of being repeatedly, anomalously missed by thunderstorms, even if accurate in a limited sense, do not mean that their locations do not receive their fair share of thunderstorms over the long run.

5. IMPORTANT IMPLICATIONS

The data and methods we used are, together, one step toward understanding anecdotal claims about weather holes and hot spots. More generally, and much more importantly, such data and methods may also prove to be very powerful tools for forecasting thunderstorms and

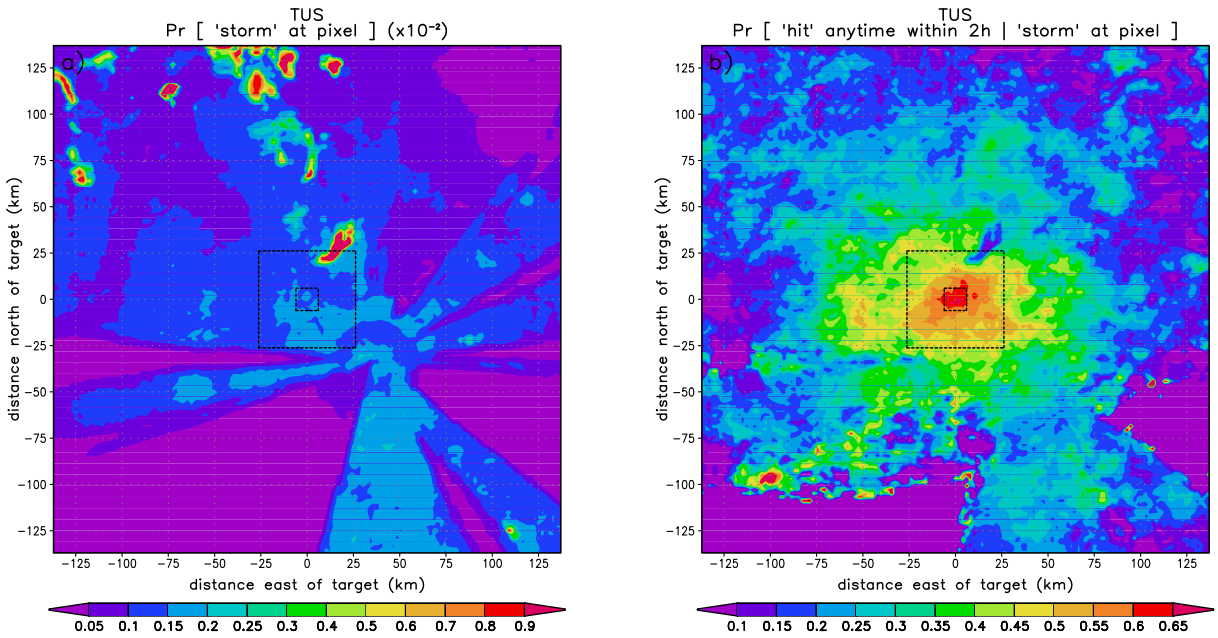

Figure 7: Same as Fig. 2 except for Tucson, Arizona.

for quantifying the risks they pose to society.

For many decades, researchers have proposed and sometimes demonstrated that climatic statistics can be a valuable tool for meteorologic and hydrologic forecasting (e.g. Kincer, 1916; Reap and Foster, 1979; Balling, 1985; Matthews and Geerts, 1995; Krzysztofowicz and Sigrest, 1997). In decades past, efforts to apply radar-derived statistics to forecasts of thunderstorms were sometimes problematic. However, the WSR-88D network is a great improvement over earlier radars, and every day WSR-88D databases grow. As they do, the statistical significance of the patterns in even small subsets of the data also grow. In the future it should be possible to construct probabilistic, short-term forecasts of thunderstorm evolution and motion by using previous storms as analogues. In addition, a sufficiently large database should allow us to stratify statistical forecasts by factors such as time of year, time of day, climate indices, synoptic wind patterns, and soil moisture. Currently, forecasters can use a few minutes of real-time radar data to track thunderstorms and predict their locations. Perhaps before long, forecasters might use decades of historic radar data not only to track extant cells, but also to predict changes in those cells' strengths and direction as well as to predict where new cells will develop.

REFERENCES

Augustine, J. A., and K. W. Howard, 1991: Mesoscale convective complexes over the United States during 1986 and 1987. *Mon. Wea. Rev.*, **119**, 1575–1589.

Balling, R. C., Jr., 1985: Warm season nocturnal precipitation in the Great Plains of the United States. *J. Climate Appl. Meteor.*, **24**, 1383–1387.

Byers, H. R., and H. R. Rodebush, 1948: Causes of thunderstorms of the Florida Peninsula. *J. Meteor.*, **5**, 275–280.

Changnon, S. A., and F. A. Huff, 1986: The urban-related nocturnal rainfall anomaly at St. Louis. *J. Climate Appl. Meteor.*, **25**, 1985–1995.

Frank, N. L., P. L. Moore, and G. E. Fisher, 1967: Summer shower distribution over the Florida peninsula as deduced from digitized radar data. *J. Appl. Meteor.*, **6**, 309–316.

Kincer, J. B., 1916: Daytime and nighttime precipitation and their economic significance. *Mon. Wea. Rev.*, **44**, 628–633.

Krzysztofowicz, R., and A. A. Sigrest, 1997: Local climate guidance for probabilistic quantitative precipitation forecasting. *Mon. Wea. Rev.*, **125**, 305–316.

Maddox, R. A., K. W. Howard, D. L. Bartels, and D. M. Rodgers, 1986: Mesoscale convective complexes in the middle lattitudes. *Mesoscale Meteorology and Forecasting*, P. S. Ray, Ed. Amer. Meteor. Soc., 390–413.

Matthews, C., and B. Geerts, 1995: Characteristic thunderstorm distribution in the sydney area. *Aust. Met. Mag.*, **44**, 127–138.

Reap, D. M., and D. S. Foster, 1979: Automated 12–36 hour probability forecasts of thunderstorms and severe local storms. *J. Appl. Meteor.*, **18**, 1304–1315.

Rozoff, C. M., W. R. Cotton, and J. O. Adegoke, 2003: Simulations of St. Louis, Missouri, land use impacts on thunderstorms. *J. Appl. Meteor.*, **42**, 716–738.

APPENDIX

Table 1: Twenty-one target sites selected for detailed study because of their high concentration of meteorologists. The right–hand column denotes the population categories in this study to which each site belonged.

3–letter ID	location	meteorological communities	categories
ALB	Albany, NY	SUNY–Albany	ALL, GOOD
ARB	Ann Arbor, MI	Univ. Michigan	ALL, GOOD
BOU	Boulder, CO	Univ. Colorado, NCAR	ALL
CLL	College Station, TX	Texas A&M Univ.	ALL, GOOD, PLAINS
CMI	Urbana–Champaign, IL	Univ. Illinois	ALL, GOOD, PLAINS
DCA	Washington, DC	Univ. Maryland, NASA–Goddard, NOAA	ALL, GOOD
FCL	Fort Collins, CO	Colorado State Univ.	ALL
GFK	Grand Forks, ND	Univ. North Dakota	ALL, GOOD, PLAINS
HSV	Huntsville, AL	Univ. Alabama–Huntsville, NASA–Marshall	ALL, GOOD
LNK	Lincoln, NE	Univ. Nebraska	ALL, GOOD, PLAINS
LAX	Los Angeles, CA	Univ. California–Los Angeles	ALL
LBB	Lubbock, TX	Texas Tech Univ.	ALL, GOOD, PLAINS
MSN	Madison, WI	Univ. Wisconsin	ALL, GOOD, PLAINS
OFF	Bellevue, NE	Air Force Weather Agency	ALL, GOOD, PLAINS
OUN	Norman, OK	Univ. Oklahoma, NSSL, Storm Prediction Center	ALL, GOOD, PLAINS
RDU	Raleigh–Durham, NC	North Carolina State Univ.	ALL, GOOD
SLC	Salt Lake City, UT	Univ. Utah	ALL
SEA	Seattle, WA	Univ. Washington	ALL
TLH	Tallahassee, FL	Florida State Univ.	ALL, GOOD
TUS	Tucson, AZ	Univ. Arizona	ALL
UNV	State College, PA	Pennsylvania State Univ.	ALL, GOOD

Table 2: Values of $\mathrm{Pr}_{\mathrm{storm}}$ for the 21 meteorological sites in this study. Columns, in order, are: 1) the site's three–letter identifier; 2) the site's city mean $\mathrm{Pr}_{\mathrm{storm}}$; 3) the difference between the city's mean $\mathrm{Pr}_{\mathrm{storm}}$ and the mean of the surrounding CWA; 4) the difference between the city's mean $\mathrm{Pr}_{\mathrm{storm}}$ and the mean of the surrounding CWA, expressed as a percentage of the CWA value; 5) the difference between the county's mean $\mathrm{Pr}_{\mathrm{storm}}$ and the mean of the surrounding CWA; 6) the difference between the county's mean $\mathrm{Pr}_{\mathrm{storm}}$ and the mean of the surrounding CWA, expressed as a percentage of the CWA value. Possible weather holes and hot spots are denoted by the symbols $\ominus$ and $\oplus$, respectively, in columns that exceed the thresholds given in the text. Sites with poor regional radar coverage are denoted by daggers next to their identifiers for reference. The CWA–wide averaged value of $\mathrm{Pr}_{\mathrm{storm}}$ was 2.32×10^{-3} for all 71 target points, 2.85×10^{-3} for the 54 GOOD points, and 2.92×10^{-3} for the 27 PLAINS points.

site	$\mathrm{Pr}_{\mathrm{storm}}$				
	city	city–CWA	%	county–CWA	%
ALB	2.97E-03	1.40E-04	4.9	5.00E-06	0.2
ARB	3.45E-03	$\oplus$ 3.30E-04	$\oplus$ 10.6	$\oplus$ 3.59E-04	$\oplus$ 11.5
BOU†	9.74E-04	1.17E-04	$\oplus$ 13.7	1.06E-04	$\oplus$ 12.4
CLL	3.81E-03	-2.20E-04	-5.5	$\ominus$-3.15E-04	-7.8
CMI	4.24E-03	1.08E-04	2.6	9.90E-05	2.4
DCA	3.21E-03	-6.60E-05	-2.0	2.10E-05	0.6
FCL†	1.31E-03	$\oplus$ 3.94E-04	$\oplus$ 43.2	2.13E-04	$\oplus$ 23.4
GFK	1.11E-03	-2.48E-04	$\ominus$-18.3	-1.59E-04	$\ominus$-11.7
HSV	5.11E-03	$\ominus$-2.98E-04	-5.5	$\ominus$-3.98E-04	-7.4
LAX†	6.71E-04	1.99E-04	$\oplus$ 42.2	2.15E-04	$\oplus$ 45.6
LBB	2.34E-03	-1.12E-04	-4.6	-1.50E-05	-0.6
LNK	3.32E-03	1.71E-04	5.4	2.80E-05	0.9
MSN	3.45E-03	1.39E-04	4.2	1.78E-04	5.4
OFF	3.68E-03	1.86E-04	5.3	1.88E-04	5.4
OUN	4.16E-03	-1.31E-04	-3.1	1.50E-05	0.3
RDU	4.38E-03	$\oplus$ 3.20E-04	7.9	$\oplus$ 3.06E-04	7.5
SEA†	2.11E-03	$\oplus$ 9.44E-04	$\oplus$ 81.3	$\oplus$ 8.60E-04	$\oplus$ 74.1
SLC†	8.49E-04	$\oplus$ 4.43E-04	$\oplus$ 109.1	$\oplus$ 4.43E-04	$\oplus$ 109.1
TLH	6.92E-03	$\oplus$ 3.82E-04	5.8	$\oplus$ 5.52E-04	8.4
TUS†	1.49E-03	$\oplus$ 5.05E-04	$\oplus$ 51.4	$\oplus$ 6.63E-04	$\oplus$ 67.4
UNV	2.18E-03	$\ominus$-4.27E-04	$\ominus$-16.4	-2.15E-04	-8.3

Table 3: Values of azimuthally–averaged $\mathrm{Pr}_{\mathrm{anyhit}|\mathrm{storm}}$ that divide the distribution into fourths, for each of 5 values of range, and for each of 3 data subsets. $q_{0.5}$ represents the median values, with $q_{0.75}$ and $q_{0.25}$ the upper and lower quartiles, respectively.

range	quartile	azimuthally–averaged $\mathrm{Pr}_{\mathrm{anyhit}|\mathrm{storm}}$		
		all points	good points	Plains points
20 km	$q_{0.75}$	0.73	0.73	0.75
	$q_{0.5}$	0.60	0.67	0.71
	$q_{0.25}$	0.40	0.53	0.61
40 km	$q_{0.75}$	0.63	0.66	0.71
	$q_{0.5}$	0.49	0.58	0.62
	$q_{0.25}$	0.26	0.44	0.52
60 km	$q_{0.75}$	0.59	0.61	0.63
	$q_{0.5}$	0.42	0.50	0.55
	$q_{0.25}$	0.22	0.35	0.44
80 km	$q_{0.75}$	0.50	0.54	0.55
	$q_{0.5}$	0.37	0.43	0.48
	$q_{0.25}$	0.15	0.31	0.39
100 km	$q_{0.75}$	0.46	0.47	0.49
	$q_{0.5}$	0.32	0.40	0.42
	$q_{0.25}$	0.11	0.28	0.34

Table 4: Values of $\mathrm{Pr}_{\mathrm{anyhit}|\mathrm{storm}}$ for the 21 meteorological sites in this study. Possible weather holes and hot spots are denoted by the symbols $\ominus$ and $\oplus$, respectively, in columns for which sites' values are in either the upper or lower quartile of the data (cf. Table 3), with superscripts indicating the subset(s) in which the site exceeded the thresholds: a all data points; g data from points with good regional coverage only; p data from points in the Plains only. Sites with poor regional radar coverage are denoted by daggers next to their identifiers. Sites that are included in the Plains dataset are denoted by double–daggers next to their identifiers.

site	azimuthally averaged $\mathrm{Pr}_{\mathrm{anyhit}|\mathrm{storm}}$				
	r=20 km	r=40 km	r=60 km	r=80 km	r=100km
ALB	0.67	0.52	0.42	0.33	0.32
ARB	0.66	0.56	0.49	0.38	0.42
BOU†	0.41	0.27	0.30	0.24	$\ominus^{a}$ 0.10
CLL‡	0.70	0.62	$\oplus^{a}$ 0.60	$\oplus^{a,g,p}$ 0.55	$\oplus^{a,g,p}$ 0.49
CMI‡	0.67	0.55	0.53	$\oplus^{a}$ 0.50	0.41
DCA	0.62	0.56	0.47	0.38	0.35
FCL†	$\ominus^{a}$ 0.40	$\ominus^{a}$ 0.26	$\ominus^{a}$ 0.22	$\ominus^{a}$ 0.14	0.17
GFK‡	$\ominus^{g,p}$ 0.53	$\ominus^{p}$ 0.48	$\ominus^{g,p}$ 0.32	$\ominus^{g,p}$ 0.25	$\ominus^{p}$ 0.32
HSV	0.70	$\oplus^{a,g}$ 0.68	$\oplus^{a,g}$ 0.62	$\oplus^{a}$ 0.53	$\oplus^{a,g}$ 0.47
LAX†	0.69	0.37	0.31	$\ominus^{a}$ 0.00	0.14
LBB‡	$\oplus^{a,g,p}$ 0.80	$\oplus^{a,g}$ 0.66	0.53	$\ominus^{p}$ 0.38	0.37
LNK‡	0.69	0.62	0.54	0.46	0.42
MSN‡	$\oplus^{a,g,p}$ 0.79	$\oplus^{a,g,p}$ 0.71	$\oplus^{a,g,p}$ 0.64	$\oplus^{a}$ 0.53	0.45
OFF‡	$\oplus^{a,g,p}$ 0.76	$\oplus^{a,g,p}$ 0.74	$\oplus^{a,g,p}$ 0.65	$\oplus^{a}$ 0.51	$\oplus^{a}$ 0.46
OUN‡	$\oplus^{a,g,p}$ 0.75	$\oplus^{a,g,p}$ 0.71	$\oplus^{a,g,p}$ 0.66	$\oplus^{a,g}$ 0.54	$\oplus^{a,g,p}$ 0.49
RDU	$\oplus^{a,g}$ 0.73	$\oplus^{a}$ 0.63	0.53	0.46	0.41
SEA†	0.43	$\ominus^{a}$ 0.16	$\ominus^{a}$ 0.07	$\ominus^{a}$ 0.02	$\ominus^{a}$ 0.02
SLC†	0.53	0.41	0.24	0.22	0.24
TLH	$\oplus^{a,g}$ 0.78	$\oplus^{a,g}$ 0.73	$\oplus^{a,g}$ 0.65	$\oplus^{a,g}$ 0.61	$\oplus^{a,g}$ 0.60
TUS†	0.45	0.37	0.31	0.21	0.15
UNV	0.56	0.47	0.42	0.41	0.33

NOWrad^{TM} national radar composite data were provided by the Global Hydrology Resource Center. *NOWrad^{TM}* is a registered trademark of the Weather Services International (WSI) Corporation. We appreciate comments and assistance from D. Ahijevych, L. Carey, C. Davis, R. Edwards, R. Henson, T. Lane, D. Loope, D. Pederson, D. Thompson, R. Thompson, and D. Zaras.